

## Do quarks really form diquark clusters in the nucleon?

Derek B. Leinweber

*Department of Physics and Center for Theoretical Physics, University of Maryland, College Park, Maryland 20742*  
(Received 7 July 1992; revised manuscript received 12 January 1993)

A gauge-invariant method for the investigation of scalar diquark clustering in the nucleon ground state is presented. The method focuses on a comparison of quark distributions in the nucleon with those in the  $\Delta$  baryon resonance. Recent lattice QCD calculations of these quark distribution radii are analyzed in a search for evidence of scalar diquark clustering. The analysis indicates the lattice results describe the negative squared charge radius of the neutron with little resort to hyperfine clustering between  $u$ - $d$  quark pairs. This result contrasts both quark-diquark and nonrelativistic quark models where hyperfine attraction between  $u$  and  $d$  quarks in the nucleon is argued to play a significant role. Comparison of light quark distributions in  $\Lambda^0$  and  $\Sigma^{*0}$  indicate only a small reduction of the scalar diquark distribution radius relative to the vector diquark distribution. Current lattice QCD determinations of baryon charge distributions do not support the concept of substantial  $u$ - $d$  scalar diquark clustering as an appropriate description of the internal structure of the nucleon.

PACS number(s): 13.40.Fn, 12.38.Gc, 14.20.Dh

### I. INTRODUCTION

The one-gluon-exchange potential (OGEP) has been extensively used to describe the spin-dependent interactions of constituent quarks in low-energy phenomenology since its inception [1]. Among the earliest of OGEP successes is an explanation of the negative squared charge radius of the neutron. Carlitz *et al.* focused on the spin-dependent hyperfine repulsion between the doubly represented  $d$  quarks in the neutron which naturally gives rise to a negative squared charge radius [2]. Later analyses exploited the larger OGEP hyperfine attraction acting between constituent quark pairs in a scalar spin-0 state [3,4]. In these papers, the attractive hyperfine force pulls the  $u$  quark of the neutron into the center, while the two  $d$  quarks are repelled to the periphery by the vector spin-1 repulsion of the hyperfine interaction. These more quantitative analyses were also successful in accounting for the neutron charge radius.

The success of hyperfine interactions based on single-gluon exchange led some authors to speculate that the strong attractive hyperfine interaction pairs a  $u$  and a  $d$  quark of the nucleon into a scalar diquark [5] of considerable clustering [6–11]. It is often argued that pointlike scalar diquarks naturally arise in QCD, or that scalar diquarks are energetically favored [12,13]. A factor in the popularity of diquark models is the numerical simplification of a three-body problem to a two-body problem [8,14,15]. Also, the diquark model is not without a long list of successful descriptions of low-energy hadronic phenomena. For example, diquark clustering can also explain the neutron charge radius. In this approach it is concluded that the neutron has a scalar diquark core [16]. More recently it has been argued that a quark-diquark approximation of the three-quark structure of baryons is now available which takes into account the inner structure of baryons at low energies [8]. Still others argue

that diquark models provide a natural forum for investigating deviations from SU(6) spin-flavor symmetry as low-energy phenomena is not tractable from first principles [17].

In this paper, a gauge-invariant method for the examination of scalar diquark clustering in the nucleon ground state is presented. Direct evidence indicating the absence of substantial diquark clustering of  $u$  and  $d$  quarks in low-lying baryons will be presented. Quark electric charge distribution radii are calculated from first principles in lattice regularized QCD. By examining the quark distributions in octet baryons where quarks may form scalar diquarks and comparing these distributions with the relevant decuplet baryons where quarks are predominantly paired in vector diquarks, one can determine the amount, if any, of scalar diquark clustering [18]. A central point of this paper is that it is a comparison of charge distribution radii between octet and decuplet baryons (as opposed to within the baryon octet) that reveals whether or not hyperfine interactions lead to scalar diquark clustering.

Of course this is not the first paper to refute the diquark picture of low-energy baryons. As early as 1981, an analysis of  $\pi N$  partial widths suggested that diquark configurations do not contribute appreciably to the structure of low-lying resonances [19]. More recently, it has been argued that pointlike scalar diquarks are unlikely in a relativistic bound-state quark model [20], and that there is no clear indication of diquark clustering in a nonrelativistic quark model of the nucleon [21].

In some systems there is good reason to believe that some diquark clustering can occur. For example, in  $\Xi$  the two strange quarks are more localized due to their heavier mass [22]. In high angular momentum systems, small attraction between quarks can lead to clustering [21]. However, the scalar diquark clustering argued to arise from the attractive part of the hyperfine interaction is not reproduced in the nonperturbative analysis presented here.

In Sec. II A, descriptions of the neutron charge radius in a quark-diquark model, a nonrelativistic constituent quark model, and lattice QCD calculations are compared. The purpose of this section is to illustrate that the three different approaches lead to values for the neutron-to-proton charge radius ratio which are consistent with each other and that the lattice results are not inconsistent with the experimentally determined value. The conclusion of this section is that reproduction of the neutron-to-proton charge radius ratio alone is insufficient to discriminate between the various quark distribution pictures. Section II B introduces the charge distributions in  $\Delta$  to discriminate between these three different descriptions of quark distributions in the nucleon. Here the absence of significant scalar diquark clustering in the lattice results is discussed. Section III explores charge distributions in  $\Lambda^0$  and  $\Sigma^{*0}$  hyperons. A similar analysis indicates the absence of substantial scalar diquark clustering in these hyperons. Section IV considers the possible sources of systematic uncertainty in the lattice calculations and how these uncertainties may affect the charge distribution radii used in this analysis. Finally the implications of the results are discussed and summarized in Sec. V.

## II. SCALAR DIQUARK CLUSTERING IN THE NUCLEON

### A. The neutron charge radius

To investigate the issue of scalar diquark clustering, we turn to the lattice investigations of baryon electromagnetic structure of Ref. [22,23]. These lattice results are obtained in a numerical simulation of quenched QCD on a  $24 \times 12 \times 12 \times 24$  lattice at  $\beta = 5.9$  using Wilson fermions. Twenty-eight gauge configurations are used in the analysis. Charge radii are obtained from lattice calculations of electromagnetic form factors at  $q^2 = 0.16 \text{ GeV}^2$ . The  $Q^2$  dependence of the form factors is taken as a dipole form. However, monopole or linear forms yield similar radii which agree with the dipole results within statistical uncertainties. A third-order, single elimination jackknife [24,25] is used to determine the statistical uncertainties in the lattice results. These uncertainties are indicated in parentheses describing the uncertainty in the last digit(s) of the results.

The lattice results have displayed some of the qualitative features expected from hyperfine interactions. Let us first focus on the mean-square charge radius of the neutron as described by the quark-diquark model [16], the nonrelativistic quark model [3,4], and the lattice simulations of Ref. [22,23]. The diquark description of quark distributions is as illustrated in Fig. 1(a). A  $u$  and a  $d$  quark form a scalar diquark cluster whose radius in extreme cases may be taken to be pointlike. The second  $d$  quark has a larger charge distribution radius and provides the required negative charge at large radii surrounding a positive core of charge  $+1/3$ .

In the nonrelativistic quark model a similar scalar diquark clustering occurs between  $u$  and  $d$  quarks due to the attractive part of the hyperfine interaction. However,

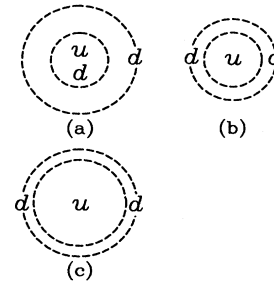


FIG. 1. Sketches of quark distribution radii in the neutron as described by (a) the quark-diquark model, (b) the non-relativistic quark model, and (c) the lattice investigations of baryon electromagnetic form factors. The dashed lines are representative of the rms charge radius of the quark distributions normalized to unit charge.

this clustering is relatively small compared to the clustering anticipated in diquark models. The remaining  $d$  quark is driven to the periphery of the neutron by the repulsive part of the hyperfine interaction. The clustering is averaged over the two  $d$  quarks of the neutron and the quark distributions may be described as in Fig. 1(b). An important point to note is that the hyperfine interaction causes *two* alterations to the unperturbed wave function. The attraction between the  $u$  and  $d$  quarks causes the whole nucleon to shrink and the repulsion between the two  $d$  quarks introduces the required asymmetry between the quark distributions to reproduce the neutron charge radius.

In understanding the results of the lattice investigation the negative mean-square charge radius of the neutron was attributed to hyperfine repulsion between the doubly represented  $d$  quarks without resorting to any hyperfine attraction [22,26]. This argument is similar to the original explanation provided by Carlitz *et al.* [2]. Of course it is the hyperfine *attraction* that is argued to naturally give rise to scalar diquark clustering in the nucleon. The current picture of quark distributions within the neutron is described as in Fig. 1(c). The difference between Figs. 1(b) and 1(c) is the possible absence of any hyperfine attraction between  $u$  and  $d$  quarks. Of course the lattice results for the neutron charge radius alone may also be consistent with either of the previous two descriptions [27].

The presence of two degrees of freedom, namely the matter radius and the charge asymmetry, allow these three different descriptions of quark distributions within the neutron to lie in quantitative agreement when reproducing the neutron-to-proton charge radius ratio. Experimental measurements [28,29] of nucleon mean-square charge radii produce a ratio of

$$\frac{\langle r^2 \rangle_n}{\langle r^2 \rangle_p} = -0.167(7). \quad (1)$$

The quark-diquark prediction of the mean-square neutron-to-proton charge radius ratio is

$$\frac{\langle r^2 \rangle_n}{\langle r^2 \rangle_p} = -0.137(9), \quad (2)$$

when the parameter of the model is fixed by previous analyses [16]. Similarly the configuration mixing induced by hyperfine interactions in the nonrelativistic quark model [3] leads to the result

$$\frac{\langle r^2 \rangle_n}{\langle r^2 \rangle_p} = -0.13. \quad (3)$$

Present lattice simulations calculate hadron properties at relatively heavy current quark masses due to the increasing computational demands encountered in inverting the fermion matrix as the quarks become lighter. In Refs. [22,23] charge radii are determined at three values of the Wilson hopping parameter  $\kappa = 0.152, 0.154,$  and  $0.156$ , corresponding to current quark masses ranging from the strange current quark mass  $m_s$  through to  $m_s/2$ . To make contact with the physical world the lattice results are extrapolated, usually linearly as a function of  $1/\kappa$  which is proportional to the current quark mass or  $m_\pi^2$ , to the point at which the physical pion mass is reproduced. Results from chiral perturbation theory [30–32] suggest that logarithmic terms divergent in the limit  $m_\pi \rightarrow 0$  should be included in the analytic structure of the nucleon charge radius extrapolation function, in addition to terms linear in  $m_\pi^2$  and other higher-order terms finite in the chiral limit. However, the physics of light pions giving rise to the divergent logarithmic term is not included in either of the quark models considered here. To allow a comparison with these models on a more equal footing, the lattice extrapolations of charge radii are done linearly in  $m_\pi^2$ , effectively subtracting the nonanalytic contributions associated with light pion dressings from the charge radii. For linear extrapolations, the difference between extrapolations of quantities to the physical pion mass as opposed to  $m_\pi = 0$  are negligible. In the following, radii are extrapolated to  $\kappa_{cr} = 0.1598(2)$  where the pion mass vanishes.

The neutron charge radius is sensitive to gluonic degrees of freedom and the lattice ratio has a large statistical error associated with it. However, it is important to demonstrate that the lattice result is consistent with the previous analyses. The lattice results indicate [23]

$$\frac{\langle r^2 \rangle_n}{\langle r^2 \rangle_p} = -0.11 \begin{pmatrix} +0.10 \\ -0.14 \end{pmatrix}. \quad (4)$$

The qualitative features of the neutron charge radius anticipated by hyperfine interactions are reproduced in each of the calculations considered. Obviously, reproduction of the neutron-to-proton charge radius ratio alone is not sufficient to determine whether it is hyperfine attraction, repulsion, or a combination of the two that is actually responsible for giving rise to the neutron charge radius. If attraction plays a significant role, then diquark-clustering models may capture the essential features of the underlying quark-gluon dynamics. On the other hand, if the lattice results indicate hyperfine attraction

does not play a significant role in determining the charge distributions then the realization of diquark clustering in the nucleon ground state is doubtful.

## B. Charge distributions in $\Delta$

To discriminate between these three different descriptions of quark distributions within the nucleon we must turn to another system where the attractive part of the hyperfine interaction does not play a significant role, i.e., the  $\Delta$  baryon resonance. By examining the changes in the quark distributions as the spin of the singly represented quark is set symmetric with the doubly represented quarks, we can investigate the relevance of scalar diquark clustering and search for the anticipated effects of one-gluon-exchange hyperfine interactions on the quark distributions.

Consider the quark distributions within the proton and how they will change in going from  $p$  to  $\Delta^+$ . Figure 2 illustrates the three previous scenarios for the proton as well as the quark distributions in  $\Delta^+$ . Hyperfine interactions are not expected to give rise to vector diquark clustering. Both the nonrelativistic quark model and the lattice results describe the  $\Delta^+$  charge distribution as a sum of three equivalent quark distributions. In fact the symmetry of the  $\Delta$  three-point correlation function demands the quark distribution radii in  $\Delta$  to be equal under SU(2) isospin symmetry. This symmetry is manifest without resorting to actual calculations on the lattice [23].

In the quark-diquark model the scalar diquark cluster is lost in  $\Delta^+$  and the net positive charge of the cluster in the nucleon moves to larger radii. For pointlike diquarks the net effect is huge, resulting in a much larger charge radius for  $\Delta^+$  than for the proton. Moreover, both  $u$ - and  $d$ -quark charge distributions swell in  $\Delta$  due to the breakup of the (pointlike)  $u$ - $d$  quark cluster. Unfortunately, quantification of these statements does not appear to be possible. A comparison of  $p$  and  $\Delta^+$  charge radii in a diquark model does not appear to have been considered. Some form factors of octet and decuplet baryons were re-

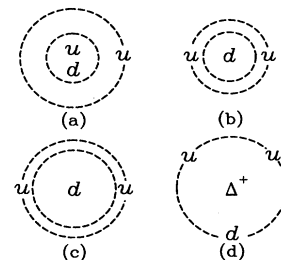


FIG. 2. Sketches of quark distribution radii in the proton as described by (a) the quark-diquark model, (b) the non-relativistic quark model, and (c) the lattice investigations of baryon electromagnetic form factors. (d) An illustration of the quark distributions in  $\Delta^+$ . The dashed lines are representative of the rms charge radius of the quark distributions normalized to unit charge.

cently examined in the quark-diquark approximation [8], however electric form factors and charge radii for  $\Delta$  resonances were not reported. To estimate a lower bound for the size of these anticipated quark distribution swellings, we refer to the nonrelativistic quark model where the role of hyperfine attraction plays a much weaker and less dramatic role.

In the nonrelativistic quark model, both the  $u$ - and  $d$ -quark distributions become broader as the attraction between  $u$  and  $d$  quarks is replaced by hyperfine repulsion in  $\Delta$ . In the model of Isgur-Karl-Koniuk [3] the predicted increase in the rms charge radius is [33,34]

$$\frac{r_{\Delta}}{r_p} = 1.28, \quad (5)$$

with the quark distributions experiencing a large swelling of

$$\frac{r_{\Delta}^u}{r_p^u} = 1.33, \quad \frac{r_{\Delta}^d}{r_p^d} = 1.49. \quad (6)$$

In the scenario previously introduced for the lattice results, the dominant effect will be the new hyperfine repulsion experienced by the  $d$  quark from the two  $u$  quarks in  $\Delta^+$ . Similarly, the two  $u$  quarks already experiencing some hyperfine repulsion will feel additional repulsion from the single  $d$  quark. Hence the dominant effect will be the broadening of the negatively charged  $d$ -quark distribution compensated by some broadening of the  $u$ -quark distribution. In fact, the lattice results suggest that the  $\Delta^+$  charge radius may actually be *smaller* than that of the proton

$$\frac{r_{\Delta}}{r_p} = 0.97(7). \quad (7)$$

This result differs by four standard deviations from the prediction of the nonrelativistic quark model. The quark distribution radii indicate the dominant effect in the lattice results is the broadening of the negatively charged  $d$ -quark distribution

$$\frac{r_{\Delta}^u}{r_p^u} = 1.01(9), \quad \frac{r_{\Delta}^d}{r_p^d} = 1.12(16). \quad (8)$$

The striking difference between the lattice results and the two models considered here is *the absence of any significant change in the lattice  $u$ -quark distribution radius*. In both models, the  $u$ -quark distribution was predicted to be broader in  $\Delta$ , largely due to the disappearance of scalar diquark clustering in going from the nucleon to

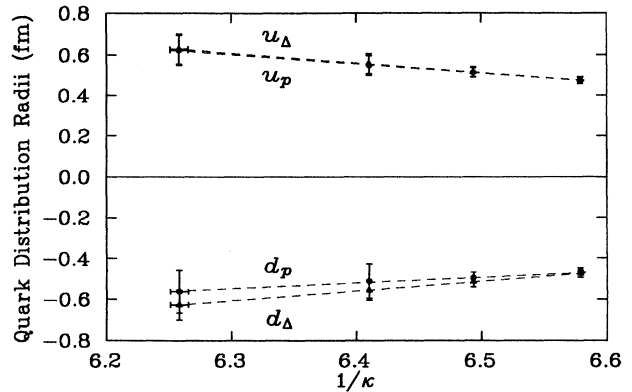


FIG. 3. Extrapolation of quark distribution radii in  $p$  and  $\Delta$  calculated at the three (rightmost) values of  $\kappa$  to  $\kappa_{\text{cr}}$  where  $m_{\pi}$  vanishes. In this and the following figure, the lattice radii ( $r/a$ ) have been scaled by a constant lattice spacing of  $a = 0.128$  fm determined from the nucleon mass. For clarity, the  $u$ -quark radii are normalized to unit charge and  $d$ -quark radii are normalized to negative unit charge. The  $u$ -quark distribution radii in  $p$  and  $\Delta$  are nearly identical at each value of  $\kappa$ .

$\Delta$ . The lattice results indicate that hyperfine attraction does not lead to substantial scalar diquark clustering in the nucleon ground state [35].

Figure 3 illustrates the extrapolation of quark distribution radii in  $p$  and  $\Delta^+$  used to obtain the results of (8). The  $u$ -quark distribution radii in  $p$  and  $\Delta$  are nearly identical for each  $\kappa$  considered. Table I details the charge distribution radii for  $p$  and  $\Delta$  and their residing quarks.

### III. SCALAR DIQUARK CLUSTERING IN $\Lambda^0$

Another place to search for evidence of scalar diquark clustering is in the charge distribution radius of the light  $u$  and  $d$  quarks in  $\Lambda^0$ . In simple quark models these quarks are generally taken as a pure scalar diquark. In other words, in this approximation the  $\Lambda^0$  magnetic moment is given by the intrinsic magnetic moment of the strange quark alone. The lattice results suggest that the  $u$  and  $d$  quarks do not form a *pure* scalar diquark and may actually contribute to the  $\Lambda^0$  magnetic moment at the level of 10%. However, for the present purpose we will ignore such effects.

In the decuplet  $\Sigma^{*0}$  hyperon state the  $u$ - $d$  sector will be

TABLE I. rms charge distribution radii normalized to unit charge in lattice units  $\langle r^2/a^2 \rangle^{1/2}$ .

Baryon	$\kappa_1 = 0.152$	$\kappa_2 = 0.154$	$\kappa_3 = 0.156$	$\kappa_{\text{cr}} = 0.1598(2)$
$p$	3.70(13)	4.04(18)	4.39(33)	5.06(48)
$\Delta^+$	3.71(13)	4.02(19)	4.34(39)	4.90(57)
$u_p$	3.69(12)	4.00(18)	4.28(38)	4.86(57)
$u_{\Delta^+}$	3.71(13)	4.02(19)	4.34(39)	4.90(57)
$d_p$	3.63(14)	3.86(21)	3.99(66)	4.39(82)
$d_{\Delta^+}$	3.71(13)	4.02(19)	4.34(39)	4.90(57)

TABLE II. rms charge distribution radii normalized to unit charge in lattice units  $\langle r^2/a^2 \rangle^{1/2}$ .  $l_\Lambda$  indicates the combined light  $u$  and  $d$  quarks in  $\Lambda^0$  and similarly for  $\Sigma^{*0}$ .

Baryon	$\kappa_1 = 0.152$	$\kappa_2 = 0.154$	$\kappa_3 = 0.156$	$\kappa_{\text{cr}} = 0.1598(2)$
$l_\Lambda$	3.65(13)	3.94(18)	4.18(44)	4.67(73)
$l_{\Sigma^*}$	3.71(13)	4.03(18)	4.40(33)	4.99(48)
$s_\Lambda$	3.70(13)	3.66(15)	3.59(22)	3.51(29)
$s_{\Sigma^*}$	3.71(13)	3.68(14)	3.65(20)	3.60(28)

paired predominately as a vector diquark. Hence, with the assumption that the  $s$  quark plays a spectator role, comparison of the light quark sector distribution radii in  $\Lambda^0$  and  $\Sigma^{*0}$  will give some indication of the relevance of scalar diquark clustering. If a scalar diquark is “dissolved” in going from  $\Lambda^0$  to  $\Sigma^{*0}$ , a broadening of the light quark distribution in  $\Sigma^{*0}$  is expected. The ratio of the light quark distributions from the lattice analyses [22,23] indicates

$$\frac{r_{\Sigma^{*0}}^l}{r_\Lambda^l} = 1.04(10), \quad (9)$$

confirming the conclusions based on the N- $\Delta$  quark distributions. Once again substantial diquark clustering is not seen.

Figure 4 illustrates the extrapolation of quark distribution radii in  $\Lambda$  and  $\Sigma^{*0}$  used to obtain the results of (9). The strange quark appears to play a satisfactory spectator role. Little change is seen between the combined light quark distributions of  $\Lambda$  and  $\Sigma^{*0}$  at each value of  $\kappa$ . Numerical values and statistical uncertainties for these radii are summarized in Table II.

#### IV. SYSTEMATIC UNCERTAINTIES

This comparison of charge distributions in octet and decuplet baryons has revealed remarkable differences be-

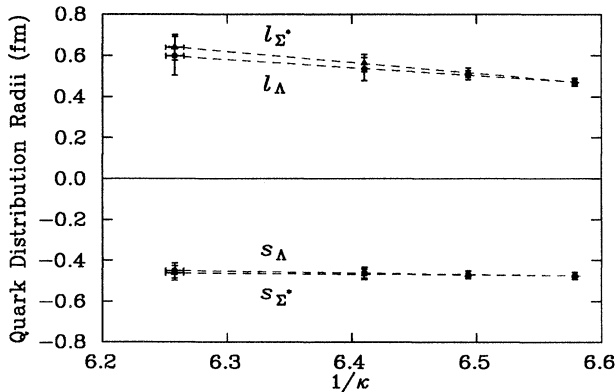


FIG. 4. Extrapolation of quark distribution radii in  $\Lambda^0$  and  $\Sigma^{*0}$ . The distribution radius of the combined light  $u$  and  $d$  quarks of  $\Lambda^0$  are denoted by  $l_\Lambda$  and similarly for  $\Sigma^{*0}$ . The light quark radii are normalized to unit charge and strange-quark radii are normalized to negative unit charge. For each  $\kappa$ ,  $l_\Lambda \simeq l_{\Sigma^*}$  indicating the absence of significant scalar diquark clustering.

tween the lattice results and the anticipated role of hyperfine attraction based on the OGEP. Moreover, this analysis appears to render a diquark picture of quark distributions in the nucleon ground state obsolete. As a result, it is important to consider the possible sources of systematic uncertainty in the lattice calculations. Systematic uncertainties may have their origin in the quenched approximation, the extrapolation of the lattice results to the physical regime, finite-volume effects or renormalization group scaling deviations.

It is worth noting that all of the lattice results presented to this point have involved ratios of lattice results. It is expected that the effects of these possible sources of systematic uncertainty will be suppressed in taking ratios. For example, while the absolute values of the lattice predictions of magnetic moments [22] are small compared to the experimentally measured values, the lattice results predict ratios of the baryon magnetic moments to the proton moment as good as or better than models, which in most cases have parameters tuned to reproduce the experimental moments. A more detailed discussion of systematic uncertainties follows.

A calculation of electromagnetic form factors in full QCD has not been done. However, at the present values of quark mass investigated on the lattice, hadron spectrum analyses suggest the dominant new physics in full QCD is a simple renormalization of the strong-coupling constant. It is possible that over large distances the quenched approximation does not screen quark interactions as much as required by full QCD. However given the similarity of the quark distribution radii discussed in this paper it is unlikely that there would be significant deviations from the results presented here.

The extrapolation of the results to the physical regime is another source of concern. However, the arguments based on the extrapolated results are supported at each value of quark mass investigated on the lattice as indicated in Tables I and II. Because the actual lattice calculations are done with  $u$ - and  $d$ -current-quark masses the order of the strange-current-quark mass, one might be concerned that hyperfine interactions such as those of the OGEP are suppressed in the lattice calculations to the point that one has no hope of observing diquark clustering. Fortunately, this is unlikely to be the case.

To assess this issue more quantitatively, one can resort to the one-gluon-exchange hyperfine interaction term which is inversely proportional to the product of quark masses. An important point is that the OGEP has some relevance only in phenomenology where constituent quark masses are used in the hyperfine term. While the current quark masses used in this investigation are some-

what heavy, the corresponding constituent quark masses are not too different from that used in phenomenology. Perhaps the easiest way to quantify this is to estimate the constituent quark mass to be  $\frac{1}{3}$  the lattice proton mass. At the lightest quark mass considered on the lattice, the constituent quark mass is approximately 430 MeV, which is not too different from the value obtained from the physical mass at 313 MeV. If the hyperfine term of the one-gluon-exchange interaction is relevant, then the differences in the strength of the hyperfine interactions for these two quark masses are within a factor of 2. For the intermediate quark mass value the strength is within a factor of 2.5. Hence, there is good reason to believe an extrapolation to the physical value is adequate. Moreover, significant mass splitting is observed between the nucleon and  $\Delta$  on the lattice where  $M_N/M_\Delta = 0.87(8)$ . However, the change in the  $u$ -quark distribution radius remains negligible. Perhaps it is also worth noting that single-gluon-exchange interaction strengths between current quarks in this lattice QCD calculation exceed the strengths common to phenomenological analyses by an order of magnitude for the lightest quark mass investigated on the lattice.

It has been argued in the past that the finite volume of the lattice may affect the lattice results, as surrounding periodic images of the baryon under study may restrict the baryon's size [22]. Note however, the  $u$ -quark distribution in  $\Delta$  is not the broadest quark distribution seen on the lattice. In addition, similar effects are seen for heavier quark masses where the quarks are more localized and less sensitive to the boundaries of the lattice. For a given value of  $\kappa$ , the charge distribution radii calculated on the lattice tend to be similar in size. For this reason the finite volume of the lattice is more likely to affect the lattice results in a global manner. For the case of a scalar  $u$ - $d$  diquark cluster in  $p$  breaking up in  $\Delta^+$ , a finite-volume effect could not simultaneously accommodate a swelling of the  $d$ -quark distribution and yet restrict the  $u$ -quark distribution from following a similar swelling.

The issue of deviations from asymptotic scaling is difficult to assess quantitatively since a similar calculation at finer lattice spacings has not been done. Toussaint [36] has demonstrated that the nucleon to  $\rho$  mass ratio calculated at  $m_\pi/m_\rho = 0.6$  is, to a good approximation, independent of the value of  $\beta$  over a range of  $\beta = 5.7$ – $6.3$  for quenched Wilson fermion calculations. Furthermore, Yoshie *et al.* [37] have demonstrated that it is possible to reproduce the hadron spectrum in quenched QCD at  $\beta = 6.0$  within statistical uncertainties of approximately 10% [36].

The lattice prediction of the current investigation for the  $\Delta/N$  mass ratio lies 12% or  $1.4\sigma$  below the experimental ratio. One could adjust the parameters of the nonrelativistic quark model to reproduce the lattice  $N$ - $\Delta$  splitting in which case the difference between the lattice and model predictions for baryon charge radii is reduced to  $2\sigma$ . However, the trend of the lattice results indicates that a doubling of the effects seen in the lattice results only widens the gap between the predictions of  $\Delta^+/p$  charge radii ratios and leaves the change in the  $u$ -quark radius in going from  $p$  to  $\Delta^+$  at the order of 2%.

## V. DISCUSSION AND SUMMARY

Faced with the discrepancies of these models which both lack mesonic degrees of freedom it is interesting to consider models such as the cloudy bag [38], or hedgehog models such as the Skyrmion [39], hybrid (or little) bag [40], and the chiral-quark meson model [41]. In hedgehog models, the proton and  $\Delta^+$  radii are equal by construction. The difference in charge radii are  $1/N_c$  suppressed and cannot be calculated using conventional semiclassical techniques. It may be useful to note that the lattice results suggest that such higher-order effects may be small.

A calculation of the charge radii considered here in the cloudy bag model could provide further insight into the importance of mesonic degrees of freedom in describing baryon charge distributions. Since a large part of the neutron charge radius has its origin in the pion cloud of the cloudy bag model [42,43], it may be possible to circumvent the problems encountered here with hyperfine interactions. Of course, to allow a direct comparison with the lattice results and to avoid problems associated with open-channel physics, the cloudy bag analysis should be done with heavier pions. The  $\Delta^+$  charge radius and internal quark distributions provide new additional information on the spin dependence of quark interactions. The traditional models examined here do not reproduce the lattice results and a description of these phenomena remains an open challenge to models of QCD.

Some have argued the existence of scalar diquarks based on large momentum transfer phenomenology. An analysis of scalar and vector diquarks at large momentum transfers in lattice QCD may provide useful insight. The results presented here may be of interest to those investigating large  $Q^2$  phenomena using nucleon ground-state wave functions as a model input representing the nonperturbative parts of the calculation [9,44].

Finally, a few comments on the absence of significant quark clustering in the lattice results relative to that anticipated by quark models are in order. The first and most obvious comment to make is that baryon charge distributions are sensitive to the long-distance nonperturbative aspects of QCD. It should not be too surprising to find that hyperfine interactions based on a single-gluon-exchange become virtually irrelevant in the nonperturbative regime. It is well known that the one-gluon-exchange hyperfine interaction has some relevance only when the quark masses are taken to be constituent quark masses. Experimental mass splittings indicate it is not the relevant interaction between current quarks. There is an infinite class of multiple-gluon-exchange diagrams to consider beyond the exchange of a single gluon. Moreover, these diagrams are equally important since the theory is nonperturbative.

A second and possibly more interesting point concerns the spin of the singly represented quark in the nucleon. From the lattice QCD analyses of baryon magnetic moments [22,23,45], it has become clear that the behavior of the singly represented quark in octet baryons is very different from the predictions of SU(6) spin-flavor symmetry. Briefly stated the lattice results indicate that the proton moment is better described as

$$\mu_p = \frac{4}{3}\mu_u - \frac{1}{6}\mu_d, \quad (10)$$

where in constituent quark model language, the  $d$  quark has its net spin opposite that of the  $u$  quarks, about half as much as suggested by SU(6). In relation to scalar diquark clustering, the probability of finding  $u$  and  $d$  quarks paired in a spin-0 state has been reduced. Once again, the lattice results suggest that scalar diquark degrees of freedom do not provide an appropriate description of the internal quark structure of low-lying baryons.

A gauge-invariant method for the examination of scalar diquark clustering in the nucleon ground state has been presented. Results from lattice QCD describing the distributions of quarks in the baryon octet and decuplet have been analyzed in a search for evidence of scalar diquark clustering. The results presented here contrast the

predictions of the nonrelativistic quark model which has a relatively small diquark clustering compared to that demanded in quark-diquark models. The lattice results do not support the concept of substantial diquark clustering as an appropriate description of the internal structure of low-lying baryons.

#### ACKNOWLEDGMENTS

I wish to thank Zbigniew Dziembowski for stirring my interest in this subject. I also thank Wojciech Broniowski, Tom Cohen, Manoj Banerjee, Nathan Isgur, and Simon Capstick for a number of interesting and helpful discussions. Financial support from the U.S. Department of Energy under Grant No. DE-FG05-87ER-40322 is gratefully acknowledged.

- 
- [1] A. De Rújula, H. Georgi, and S. L. Glashow, *Phys. Rev. D* **12**, 147 (1975).
  - [2] R. D. Carlitz, S. D. Ellis, and R. Savit, *Phys. Lett.* **68B**, 433 (1977).
  - [3] N. Isgur, G. Karl, and R. Koniuk, *Phys. Rev. Lett.* **41**, 1269 (1978); **45**, 1738(E) (1980).
  - [4] N. Isgur, G. Karl, and D. W. L. Sprung, *Phys. Rev. D* **23**, 163 (1981).
  - [5] D. B. Lichtenberg, *Phys. Rev.* **178**, 2197 (1969).
  - [6] K. S. Sateesh, *Phys. Rev. D* **45**, 866 (1992).
  - [7] M. Anselmino and E. Predazzi, *Phys. Lett. B* **254**, 203 (1991).
  - [8] G. V. Efimov, M. A. Ivanov, and V. E. Lyubovitskij, *Z. Phys. C* **47**, 583 (1990).
  - [9] Z. Dziembowski and J. Franklin, *Phys. Rev. D* **42**, 905 (1990).
  - [10] H. G. Dosch, M. Jamin, and B. Stech, *Z. Phys. C* **42**, 167 (1989).
  - [11] S. Fredriksson, *Phys. Rev. Lett.* **52**, 724 (1984).
  - [12] S. Fredriksson and T. Larsson, *Phys. Rev. D* **28**, 255 (1983).
  - [13] S. Fredriksson, M. Jändel, and T. Larsson, *Z. Phys. C* **14**, 35 (1982).
  - [14] D. B. Lichtenberg, W. Namgung, E. Predazzi, and J. G. Wills, *Phys. Rev. Lett.* **48**, 1653 (1982).
  - [15] D. B. Lichtenberg, E. Predazzi, and J. G. Wills, *Z. Phys. C* **17**, 57 (1983).
  - [16] Z. Dziembowski, W. J. Metzger, and R. T. Van de Walle, *Z. Phys. C* **10**, 231 (1981).
  - [17] T. Uppal and R. C. Verma, *Z. Phys. C* **52**, 307 (1991).
  - [18] Note that an individual quark flavor distribution radius is a gauge-invariant quantity. The radius may be regarded as a baryon charge radius in which the remaining quark flavors have zero electric charge.
  - [19] C. P. Forsyth and R. E. Cutkosky, *Nucl. Phys.* **B178**, 35 (1981).
  - [20] B. Ram and V. Kriss, *Phys. Rev. D* **35**, 400 (1987).
  - [21] S. Fleck, B. Silvestre-Brac, and J. M. Richard, *Phys. Rev. D* **38**, 1519 (1988).
  - [22] D. B. Leinweber, R. M. Woloshyn, and T. Draper, *Phys. Rev. D* **43**, 1659 (1991).
  - [23] D. B. Leinweber, T. Draper, and R. M. Woloshyn, *Phys. Rev. D* **46**, 3067 (1992).
  - [24] B. Efron, *SIAM (Soc. Ind. Appl. Math.) Rev.* **21**, 460 (1979).
  - [25] S. Gottlieb, P. B. MacKenzie, H. B. Thacker, and D. Weingarten, *Nucl. Phys.* **B263**, 704 (1986).
  - [26] T. Draper, R. M. Woloshyn, and K. F. Liu, *Phys. Lett. B* **234**, 121 (1990).
  - [27] At this point we do not have sufficient information to exclude the possibility of a significant role for hyperfine attraction in the lattice results. However, it will become clear through the analysis of  $\Delta$  baryons that hyperfine attraction does not play a significant role in determining the quark charge distribution radii.
  - [28] G. Höhler *et al.*, *Nucl. Phys.* **B114**, 505 (1976).
  - [29] O. Dumbrajs, *Nucl. Phys.* **B216**, 277 (1983).
  - [30] M. A. B. Bég and A. Zepeda, *Phys. Rev. D* **6**, 2912 (1972).
  - [31] D. B. Leinweber and T. D. Cohen, *Phys. Rev. D* **47**, 2147 (1993).
  - [32] T. D. Cohen and D. B. Leinweber, *Comments Nucl. Part. Phys.* (to be published).
  - [33] N. Isgur and G. Karl, *Phys. Rev. D* **21**, 3175 (1980).
  - [34] Here we have taken  $\theta_\Delta = -\theta_p$ , and  $\phi_\Delta = 0$ . Equation (13) of Ref. [3] has been adjusted as described in the errata.
  - [35] In the preceding arguments, the focus in the lattice scenario has been on hyperfine repulsion. However, the lattice results are also consistent with a mixture of hyperfine attraction and repulsion or even exclusive hyperfine attraction provided the clustering is small. The important point to draw from this examination of charge radii is that there is no evidence of significant  $u$ - $d$  quark clustering in the nucleon ground-state quark distributions.
  - [36] D. Toussaint, in *Lattice '91*, Proceedings of the International Symposium, Tsukuba, Japan, 1991, edited by M. Fukugita *et al.* [*Nucl. Phys. B (Proc. Suppl.)* **26** (1992)].
  - [37] T. Yoshie, Y. Iwasaki, and S. Saki, in *Lattice '91* [36].
  - [38] A. W. Thomas, in *Advances in Nuclear Physics*, edited by J. Negle and E. Vogt, Vol. 13 (Plenum, New York, 1984).
  - [39] I. Zahed and G. E. Brown, *Phys. Rep.* **142**, 1 (1986).
  - [40] L. Vepstas and A. D. Jackson, *Phys. Rep.* **187**, 109 (1990).
  - [41] M. K. Banerjee, W. Broniowski, and T. D. Cohen, in

*Chiral Solitons*, edited by K. F. Liu (World Scientific, Singapore, 1987).

- [42] S. Theberge, A. W. Thomas, and G. A. Miller, Phys. Rev. D **22**, 2838 (1980).
- [43] F. Myhrer, Phys. Lett. **110B**, 353 (1982).
- [44] H. Meyer and P. J. Mulders, Nucl. Phys. **A528**, 589 (1991).
- [45] D. B. Leinweber, Phys. Rev. D **45**, 252 (1992).